Steel and Composite Structures, *Vol. 28, No. 4 (2018) 415-426*
DOI: https://doi.org/10.12989/scs.2018.28.4.415

Vibration and buckling of laminated beams by a multi-layer finite element model

Volkan Kahya* and Muhittin Turan[a]

Department of Civil Engineering, Faculty of Engineering, Karadeniz Technical University, Trabzon 61080, Turkey

(*Received July 13, 2017, Revised January 14, 2018, Accepted June 5, 2018*)

Abstract. This paper presents a multi-layer finite element for buckling and free vibration analyses of laminated beams based on a higher-order layer-wise theory. An N-layer beam element with $(9N + 7)$ degrees-of-freedom is proposed for analyses. Delamination and slip between the layers are not allowed. Element matrices for the single- and multi-layer beam elements are derived by Lagrange's equations. Buckling loads and natural frequencies are calculated for different end conditions and lamina stacking. Comparisons are made to show the accuracy of proposed element.

Keywords: laminated beams; finite element method; free vibration; buckling; higher-order shear deformation theory

1. Introduction

Laminated composites have been increased in use due to their high strength to weight ratio and flexural rigidity. This brings increase in their applications to different branches of engineering. Many engineering structures or structural components in the field of mechanical and civil engineering are commonly modeled as laminated composite beams. Hence, it is quite essential to understand static and dynamic behavior of such structures.

There is a vast literature related to the laminated composite beams. In these works, different analytical/semi-analytical and numerical methods were used. Reddy (1997) gave analytical and numerical solutions to bending, buckling and free vibration problems of laminated composite beams and plates. In laminated beams, the effect of shear deformation is highly important. The first-order shear deformation theory (FSDT) was, thus, developed to include the effect of shear. In this theory, a constant transverse shear strain through-the-thickness was assumed, and a shear correction factor must be used. To calculate the shear correction factor accurately is cumbersome in case of material anisotropy because it depends on geometrical and elastic properties of beam. Nevertheless, FSDT has been extensively used in analysis of laminated composite beams (Yuan and Miller 1989, Teboub and Hajela 1995, Banerjee 1998, Chakraborty *et al*. 2002, Goyal and Kapania 2007, Jafari-Talookolaei *et al*. 2012, Kahya 2012, 2016).

To avoid the use of shear correction factor, various higher-order shear deformation theories (HSDT) have been developed. Some of these theories, a cubic variation of in-plane displacement components was employed to have better representation of the transverse shear stresses through-the-thickness as well as to satisfy the stress-free conditions at top and bottom surfaces of the beam (Yuan and Miller 1990, Kant *et al*. 1998, Rao *et al*. 2001, Vo and Thai 2012, Li and Qiao 2015, Mantari and Canales 2016). Matsunaga (2001) obtained natural frequencies and buckling stresses of laminated composite beams by the method of power series expansion of displacement components. Aydogdu (2005, 2006) employed parabolic, hyperbolic and exponential shear deformation theories for free vibration and buckling analyses of cross-ply laminated beams. Nguyen *et al*. (2017) developed a new trigonometric-series solution based on a higher-order theory for analysis of composite beams with arbitrary lay-ups.

The layer-wise displacement models have also been developed to analyze sandwich and laminated composite beams. In these models, the displacement fields are layer-dependent, and can provide in-plane displacement and shear stress continuity at layer interfaces (Karama *et al*. 1998, Arya 2003, Dafedar and Desai 2004, Chakrabarti *et al*. 2012, Filippi and Carrera 2016). An assessment of various displacement-based theories for vibration and buckling analyses of sandwich and laminated composite beams was presented by Zhen and Wanji (2008) with comparisons of analytical solutions.

This study presents a higher-order finite element for free vibration and buckling of laminated composite and sandwich beams. The theory considered here was first used by Yuan and Miller (1990) in the static analysis of laminated beams. According to this theory, the present N-layer element is constituted in layer-wise manner and contains $(9N + 7)$ degrees-of-freedom (DOFs). Delamination and slip between the layers are not allowed. Accuracy of the element is validated through the comparisons with the available results for buckling loads and natural frequencies of laminated beams with different end conditions and lamination scheme.

*Corresponding author, Associate Professor, E-mail: volkan@ktu.edu.tr
[a] Ph.D. Student

ISSN: 1229-9367 (Print), 1598-6233 (Online)

2. Theory

Consider a laminated beam as shown in Fig. 1. According to the theory considered here, displacements at any point in the beam are (Yuan and Miller 1990)

$$U(x,z,t)=u(x,t)-z\phi(x,t)-z^2\beta_1(x,t)-z^3\beta_2(x,t),\qquad W(x,z,t)=w(x,t) \tag{1}$$

where u, w and ϕ are the axial and transversal displacements, and cross-sectional rotation, respectively. β_1 and β_2 are the higher-order terms arising from Taylor expansion. All displacement components are measured on the neutral axis, and t is time.

The strain-displacement relations are given by

$$\varepsilon_{xx}=\frac{\partial U}{\partial x}=u_{,x}-z\phi_{,x}-z^2\beta_{1,x}-z^3\beta_{2,x},\qquad \gamma_{xz}=\frac{\partial U}{\partial z}+\frac{\partial W}{\partial x}=w_{,x}-z\phi-2z\beta_{1,x}-3z^2\beta_{2,x} \tag{2}$$

where ε_{xx} and γ_{xz} are the normal and shear strains, respectively. $(\bullet)_{,x}$ denotes the derivative with respect to x.

The constitutive relations for an orthotropic ply configuration are given by

$$\sigma_{xx}=\bar{Q}_{11}\varepsilon_{xx},\quad \tau_{xz}=\bar{Q}_{55}\gamma_{xz} \tag{3}$$

where σ_{xx} and τ_{xz} are the normal and shear stresses, respectively. $\bar{Q}_{11}$ and $\bar{Q}_{55}$ are the transformed material constants which are given by

$$\bar{Q}_{11}=Q_{11}c^4+2(Q_{12}+2Q_{66})c^2s^2+Q_{22}s^4,\qquad \bar{Q}_{55}=Q_{55}c^2+Q_{44}s^2 \tag{4}$$

where $c=\cos\alpha$, $s=\sin\alpha$ and α is the fiber angle measured from the positive x-axis in counter clockwise direction. Q_{ij} terms are

$$Q_{11}=\frac{E_{11}}{1-\nu_{12}\nu_{21}},\quad Q_{12}=\frac{\nu_{12}E_{22}}{1-\nu_{12}\nu_{21}},\quad Q_{22}=\frac{E_{22}}{1-\nu_{12}\nu_{21}},\qquad Q_{44}=G_{23},\quad Q_{55}=G_{13},\quad Q_{66}=G_{12} \tag{5}$$

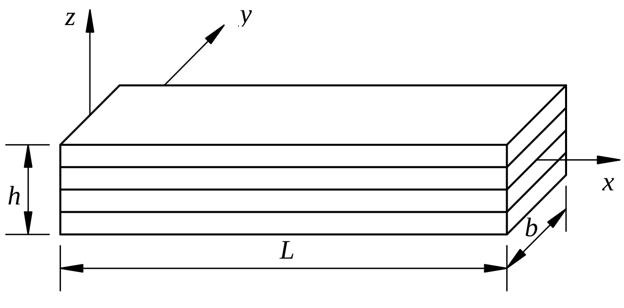

Fig. 1 Geometry and dimensions of the laminated composite beam and the coordinate system

where E_{ij} and G_{ij} denote Young's and shear modulus, respectively, ν_{ij} is Poisson ratio.

The strain energy of the beam can be given by

$$\begin{aligned}U&=\frac{1}{2}\int_0^L\int_A(\sigma_{xx}\varepsilon_{xx}+\tau_{xz}\gamma_{xz})dAdx\\&=\frac{1}{2}\int_0^L\Big\{A_0u_{,x}^2-2A_1u_{,x}\phi_{,x}+A_2\left(\phi_{,x}^2-2u_{,x}\beta_{1,x}\right)\\&\quad+2A_3\left(\phi_{,x}\beta_{1,x}-u_{,x}\beta_{2,x}\right)+A_4\left(\beta_{1,x}^2+\phi_{,x}\beta_{2,x}\right)\\&\quad+2A_5\beta_{1,x}\beta_{2,x}+A_6\beta_{2,x}^2+B_0\left(\phi^2-2\phi w_{,x}+w_{,x}^2\right)\\&\quad+4B_1\beta_1\left(\phi-w_{,x}\right)+2B_2\left(2\beta_1^2+3\phi\beta_2-3\beta_2w_{,x}\right)\\&\quad+12B_3\beta_1\beta_2+9B_4\beta_2^2\Big\}dx\end{aligned} \tag{6}$$

where

$$A_n=\int_A\bar{Q}_{11}z^ndA\ \ (n=0,1,2,\ldots,6),\qquad B_m=\int_A\bar{Q}_{55}z^mdA\ \ (m=0,1,2,3,4) \tag{7}$$

The kinetic energy can be expressed by

$$\begin{aligned}T&=\frac{1}{2}\int_0^L\int_A\rho(\dot{U}^2+\dot{W}^2)dAdx\\&=\frac{1}{2}\int_0^L\Big\{I_0\dot{u}^2-2I_1\dot{u}\,\dot{\phi}+I_2\left(\dot{\phi}^2-2\dot{u}\dot{\beta}_1\right)\\&\quad+2I_3\left(\dot{\phi}\dot{\beta}_1-\dot{u}\dot{\beta}_2\right)+I_4\left(\dot{\beta}_1^2+2\dot{\phi}\dot{\beta}_2\right)\\&\quad+2I_5\dot{\beta}_1\dot{\beta}_2+I_6\dot{\beta}_2^2+I_0\dot{w}^2\Big\}dx\end{aligned} \tag{8}$$

where dot denotes the derivative with respect to time, and

$$I_n=\int_A\rho z^ndA\ \ (n=0,1,2,\ldots,6) \tag{9}$$

In Eqs. (6) to (9), A is the cross-sectional area of the beam.

The work done by the axial compressive force P_0 acting on the beam at its ends can be given by

$$V=\frac{1}{2}\int_0^LP_0w_{,x}^2dx \tag{10}$$

3. Finite element formulation

3.1 Element matrices for a one-layer beam

Fig. 2 shows five-node beam element with four equally spaced nodes and a node at the middle. This model formerly proposed by Yuan and Miller (1990) for bending of laminated beams. It has sixteen DOFs measured on the neutral axis of the beam. The nodal displacement vector can be given by

$$\mathbf{q}=\{u_1\ \cdots\ u_3\ \ w_1\ \cdots\ w_4\ \ \phi_1\ \cdots\ \phi_3\ \ \beta_{11}\ \cdots\ \beta_{13}\ \ \beta_{21}\ \cdots\ \beta_{23}\}^T \tag{11}$$

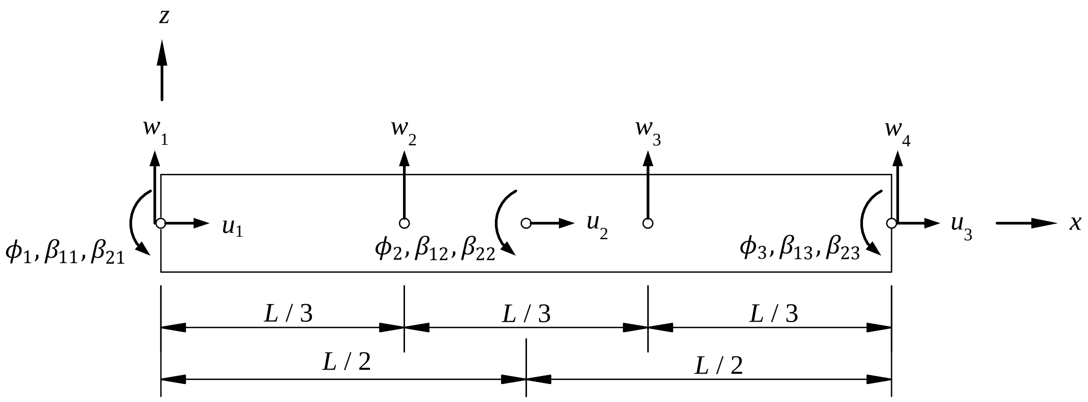

Fig. 2 One-layer beam element with sixteen degrees-of-freedom

Assume the solutions to $u(x,t)$, $w(x,t)$, $\phi(x,t)$, $\beta_1(x,t)$ and $\beta_2(x,t)$ as

$$\begin{aligned} u(x,t) &= \sum_{i=1}^{3} \varphi_i(x)\, u_i(t), \\ w(x,t) &= \sum_{i=1}^{4} \psi_i(x)\, w_i(t), \\ \phi(x,t) &= \sum_{i=1}^{3} \theta_i(x)\, \phi_i(t), \\ \beta_1(x,t) &= \sum_{i=1}^{3} \varpi_{1i}(x)\, \beta_{1i}(t), \\ \beta_2(x,t) &= \sum_{i=1}^{3} \varpi_{2i}(x)\ \beta_{2i}(t) \end{aligned} \tag{12}$$

where $\varphi_i(x)$, $\psi_i(x)$, $\theta_i(x)$, $\varpi_{i1}(x)$ and $\varpi_{i1}(x)$ are the shape functions, and $u_i(t)$, $w_i(t)$, $\phi_i(t)$, $\beta_{1i}(t)$ and $\beta_{2i}(t)$ are the generalized nodal displacements. The shape functions are chosen as

$$\begin{aligned} \varphi(x) &= c_1 + c_2 x + c_3 x^2, \\ \psi(x) &= c_4 + c_5 x + c_6 x^2 + c_7 x^3, \\ \phi(x) &= c_8 + c_9 x + c_{10} x^2, \\ \varpi_1(x) &= c_{11} + c_{12} x + c_{13} x^2, \\ \varpi_2(x) &= c_{14} + c_{15} x + c_{16} x^2 \end{aligned} \tag{13}$$

to ensure the compatibility of deformation. Selecting such a type of polynomials for the shape functions guarantees the parabolic distribution of transverse shear stresses across the thickness.

The governing equations of motion can be obtained by Lagrange's equations which is given by

$$\frac{d}{dt}\left(\frac{\partial L}{\partial \dot{q}_i}\right) - \frac{\partial L}{\partial q_i} = 0 \tag{14}$$

where $L = T - (U + V)$ is the Lagrangian functional, q_i denotes the generalized coordinates corresponding to nodal displacements given by Eq. (11). Substituting Eqs. (6), (8) and (10) into Eq. (14) with considering the solutions given by Eqs. (12) leads to

$$\mathbf{m}\ddot{\mathbf{u}} + (\mathbf{k} - P_0\, \mathbf{g})\mathbf{u} = 0 \tag{15}$$

where **m**, **k**, and **g** are, respectively, 16×16 symmetric element mass, stiffness and geometric stiffness matrices which are given in Appendix.

3.2 Multilayered beam element

When constituting the element matrices of N-layer beam element shown in Fig. 3, only rotational and higher-order DOFs are added to the system as in Yuan and Miller (1990).

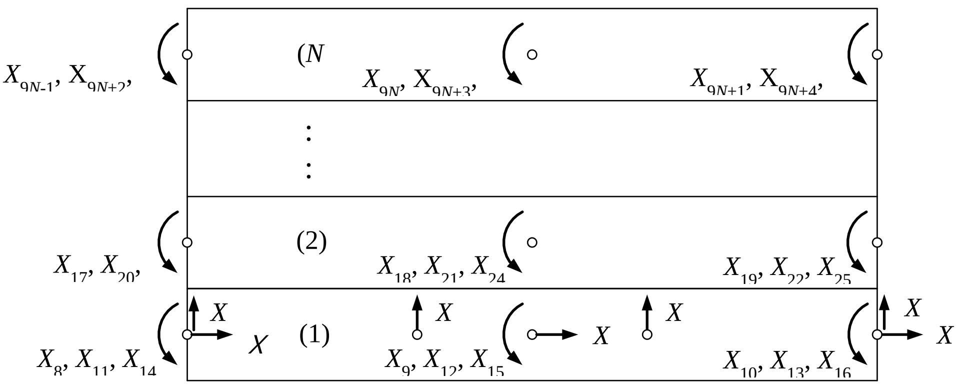

Fig. 3 Multilayered beam element

No additional axial and transversal DOF are necessary. Consequently, for the N-layer beam element, total number of DOFs is ($9N + 7$). In order to connect the kth layer to the ($k + 1$)th layer, the following kinematic constraints are used

$$
\begin{aligned}
u_1^{(k+1)} &= u_1^{(k)} - \frac{1}{2}\Big[\phi_1^{(k)} h^{(k)} - \beta_{11}^{(k)} (h^{(k)})^2 - \beta_{21}^{(k)} (h^{(k)})^3 \\
&\quad -\phi_1^{(k+1)} h^{(k+1)} + \beta_{11}^{(k+1)} (h^{(k+1)})^2 - \beta_{21}^{(k+1)} (h^{(k+1)})^3\Big], \\
u_2^{(k+1)} &= u_2^{(k)} - \frac{1}{2}\Big[\phi_2^{(k)} h^{(k)} - \beta_{12}^{(k)} (h^{(k)})^2 - \beta_{22}^{(k)} (h^{(k)})^3 \\
&\quad -\phi_2^{(k+1)} h^{(k+1)} + \beta_{12}^{(k+1)} (h^{(k+1)})^2 - \beta_{22}^{(k+1)} (h^{(k+1)})^3\Big], \\
u_3^{(k+1)} &= u_3^{(k)} - \frac{1}{2}\Big[\phi_3^{(k)} h^{(k)} - \beta_{13}^{(k)} (h^{(k)})^2 - \beta_{23}^{(k)} (h^{(k)})^3 \\
&\quad -\phi_3^{(k+1)} h^{(k+1)} + \beta_{13}^{(k+1)} (h^{(k+1)})^2 - \beta_{23}^{(k+1)} (h^{(k+1)})^3\Big]
\end{aligned}
\tag{16}
$$

$$
\begin{aligned}
w_1^{(k+1)} &= w_1^{(k)}, \quad w_2^{(k+1)} = w_2^{(k)}, \\
w_3^{(k+1)} &= w_3^{(k)}, \quad w_4^{(k+1)} = w_4^{(k)}
\end{aligned}
\tag{17}
$$

which are obtained by equating the axial and vertical displacements at the layer interfaces to ensure the continuity.

Considering Eq. (15), the load-displacement relations for each lamina can be written as

$$
\begin{aligned}
\mathbf{f}^{(N)} &= \mathbf{m}^{(N)}\ddot{\mathbf{u}}^{(N)} + (\mathbf{k}^{(N)} - P_0\,\mathbf{g}^{(N)})\mathbf{u}^{(N)}, \\
\mathbf{f}^{(N-1)} &= \mathbf{m}^{(N-1)}\ddot{\mathbf{u}}^{(N-1)} + (\mathbf{k}^{(N-1)} - P_0\,\mathbf{g}^{(N-1)})\mathbf{u}^{(N-1)}, \\
&\vdots \\
\mathbf{f}^{(1)} &= \mathbf{m}^{(1)}\ddot{\mathbf{u}}^{(1)} + (\mathbf{k}^{(1)} - P_0\,\mathbf{g}^{(1)})\mathbf{u}^{(1)}
\end{aligned}
\tag{18}
$$

where $\mathbf{f}^{(k)}$ denotes the nodal force vector which is zero here.

The local displacement vector $\mathbf{u}^{(k)}$ for each lamina can be converted to $\mathbf{X}^{(k)}$, which is a column vector with dimension ($10 + 9N$ - 3k) × 1 including the local variables of kth lamina as well as the rotational variables of the other laminae between k and N, by using the followings (Yuan and Miller 1990, Kahya 2012, 2016)

$$
\begin{aligned}
\mathbf{u}^{(N)} &= \mathbf{R}^{(N)}\mathbf{X}^{(N)}, \\
\mathbf{u}^{(N-1)} &= \mathbf{R}^{(N-1)}\mathbf{X}^{(N-1)}, \\
&\vdots \\
\mathbf{u}^{(1)} &= \mathbf{R}^{(1)}\mathbf{X}^{(1)}
\end{aligned}
\tag{19}
$$

where $\mathbf{R}^{(k)}$ is a 16 × ($16 + 9N - 9k$) matrix which is defined as

$$
\text{All } R_{ij}^{(k)} = 0 \text{ except } R_{ii}^{(k)} = 1 \ (i, j = 1-16) \tag{20}
$$

$\mathbf{X}^{(k)}$ can be converted to $\mathbf{X}^{(k\text{-}1)}$ by the following relations

$$
\begin{aligned}
\mathbf{X}^{(N)} &= \mathbf{T}^{(N-1)}\mathbf{X}^{(N-1)}, \\
\mathbf{X}^{(N-1)} &= \mathbf{T}^{(N-2)}\mathbf{X}^{(N-2)}, \\
&\vdots \\
\mathbf{X}^{(2)} &= \mathbf{T}^{(1)}\mathbf{X}^{(1)}
\end{aligned}
\tag{21}
$$

where $\mathbf{T}^{(k)}$ is a ($7 + 9N - 9k$) × ($16 + 9N - 9k$ matrix which can be obtained by Eqs. (16) and (17) as

$$
\begin{aligned}
&\text{All } T_{ij}^{(k)} = 0 \text{ except} \\
&T_{ii}^{(k)} = 1, \quad i = 1-7, \\
&T_{i(i+9)}^{(k)} = 1, \quad i = 8-(7+9N-9k), \\
&T_{i(i+7)}^{(k)} = -\frac{h^{(k)}}{2}, \ T_{i(i+10)}^{(k)} = -\left(\frac{h^{(k)}}{2}\right)^2, \\
&T_{i(i+13)}^{(k)} = -\left(\frac{h^{(k)}}{2}\right)^3, \ T_{i(i+16)}^{(k)} = -\frac{h^{(k+1)}}{2}, \\
&T_{i(i+19)}^{(k)} = \left(\frac{h^{(k+1)}}{2}\right)^2, \ T_{i(i+22)}^{(k)} = -\left(\frac{h^{(k+1)}}{2}\right)^3, \ i = 1-3
\end{aligned}
\tag{22}
$$

The local load vectors given by Eq. (18) can be transformed to the global ones by the followings

$$
\begin{aligned}
\mathbf{F}^{(1)} &= \mathbf{R}^{(1)^T}\mathbf{f}^{(1)}, \\
\mathbf{F}^{(2)} &= \mathbf{T}^{(1)^T}\mathbf{R}^{(2)^T}\mathbf{f}^{(2)}, \\
&\vdots \\
\mathbf{F}^{(N)} &= \mathbf{T}^{(1)^T}\mathbf{T}^{(2)^T}\cdots\mathbf{T}^{(N-1)^T}\mathbf{R}^{(N)^T}\mathbf{f}^{(N)}
\end{aligned}
\tag{23}
$$

Combining Eqs. (18), (19), (21) and (23) gives the final expressions for the element matrices of the multilayered beam element as follows

$$
\begin{aligned}
\bar{\mathbf{M}} &= \mathbf{R}^{(1)T}\mathbf{m}^{(1)}\mathbf{R}^{(1)} + \mathbf{T}^{(1)T}(\mathbf{R}^{(2)T}\mathbf{m}^{(2)}\mathbf{R}^{(2)} \\
&\quad + \mathbf{T}^{(2)T}(\mathbf{R}^{(3)T}\mathbf{m}^{(3)}\mathbf{R}^{(3)} + \ldots \\
&\quad + \mathbf{T}^{(N-2)T}(\mathbf{R}^{(N-1)T}\mathbf{m}^{(N-1)}\mathbf{R}^{(N-1)} \\
&\quad + \mathbf{T}^{(N-1)T}\mathbf{m}^{(N)}\mathbf{T}^{(N-1)})\mathbf{T}^{(N-2)})\ldots)\mathbf{T}^{(2)})\mathbf{T}^{(1)}, \\
\bar{\mathbf{K}} &= \mathbf{R}^{(1)T}\mathbf{k}^{(1)}\mathbf{R}^{(1)} + \mathbf{T}^{(1)T}(\mathbf{R}^{(2)T}\mathbf{k}^{(2)}\mathbf{R}^{(2)} \\
&\quad + \mathbf{T}^{(2)T}(\mathbf{R}^{(3)T}\mathbf{k}^{(3)}\mathbf{R}^{(3)} + \ldots \\
&\quad + \mathbf{T}^{(N-2)T}(\mathbf{R}^{(N-1)T}\mathbf{k}^{(N-1)}\mathbf{R}^{(N-1)} \\
&\quad + \mathbf{T}^{(N-1)T}\mathbf{k}^{(N)}\mathbf{T}^{(N-1)})\mathbf{T}^{(N-2)})\ldots)\mathbf{T}^{(2)})\mathbf{T}^{(1)}, \\
\bar{\mathbf{G}} &= \mathbf{R}^{(1)T}\mathbf{g}^{(1)}\mathbf{R}^{(1)} + \mathbf{T}^{(1)T}(\mathbf{R}^{(2)T}\mathbf{g}^{(2)}\mathbf{R}^{(2)} \\
&\quad + \mathbf{T}^{(2)T}(\mathbf{R}^{(3)T}\mathbf{g}^{(3)}\mathbf{R}^{(3)} + \ldots \\
&\quad + \mathbf{T}^{(N\text{-}2)T}(\mathbf{R}^{(N\text{-}1)T}\mathbf{g}^{(N\text{-}1)}\mathbf{R}^{(N\text{-}1)} \\
&\quad + \mathbf{T}^{(N\text{-}1)T}\mathbf{g}^{(N)}\mathbf{T}^{(N\text{-}1)})\mathbf{T}^{(N\text{-}2)})\ldots)\mathbf{T}^{(2)})\mathbf{T}^{(1)}
\end{aligned}
\tag{24}
$$

3.3 Free vibration and buckling problem

Following the usual finite element procedure, we have obtained the global equation of motion for the beam shown in Fig. 1 with different end conditions as

$$\mathbf{M}\ddot{\mathbf{X}} + (\mathbf{K} - P_0\,\mathbf{G})\mathbf{X} = 0 \tag{25}$$

where **M**, **K** and **G** are the global mass, stiffness and geometric stiffness matrices, respectively. $P_0 = bh^{(k)}\sigma_{xx}^0$, where σ_{xx}^0 is the axial compressive stress acting on the beam at its ends. **X** is the nodal displacement vector including the unknowns for the *N*-layer beam.

For free vibration of the beam without axial loading, ignoring **G** matrix and assuming $\mathbf{X} = \mathbf{X}_0 e^{i\omega t}$ in Eq. (25), we have the following eigenvalue problem

$$(\mathbf{K} - \omega^2\mathbf{M})\mathbf{X}_0 = \mathbf{0} \tag{26}$$

For buckling analysis, ignoring **M** matrix and assuming $\mathbf{X} = \mathbf{X}_0 e^{\lambda x}$, the stability equation becomes

$$(\mathbf{K} - \lambda\mathbf{G})\mathbf{X}_0 = \mathbf{0} \tag{27}$$

The natural frequencies ω_n and buckling loads $\lambda = (P_0)_{cr}$ of the beam can be obtained by non-trivial solutions of Eqs. (26) and (27).

4. Numerical results

In order to show the accuracy of the present element, some illustrative examples are considered. Numerical results are obtained by means of a computer code written in FORTRAN language. Simply-supported (S-S), clamped-clamped (C-C) and clamped-free (C-F) end conditions are considered for different laminated composite and sandwich beams.

4.1 Laminated composite beams

Laminae are assumed to have the same thickness and the following material properties: (i) Material I: E_1/E_2 = open, $G_{12} = G_{13} = 0.6E_2$, $G_{23} = 0.5E_2$, $\nu_{12} = 0.25$; (ii) Material II: E_1/E_2 = open, $G_{12} = G_{13} = 0.5E_2$, $G_{23} = 0.2E_2$, $\nu_{12} = 0.25$; (iii) Material III: E_{11} = 144.8GPa, E_{22} = 9.65 GPa, $G_{12} = G_{13}$ = 4.14 GPa, G_{23} = 3.45 GPa, ν_{12} = 0.3, ρ = 1389 kg/m^3. For convenience, the following normalized terms are used:

$$\bar{\omega} = \omega L^2\sqrt{\rho/E_{22}}\,/\,h \quad \text{for Materials I and II,}$$
$$\bar{\omega} = \omega L^2\sqrt{\rho/E_{11}}\,/\,h \quad \text{for Material III}$$
$$\bar{\lambda} = \lambda L^2/(E_{22}bh^3) \quad \text{for Materials I and II,}$$
$$\bar{\lambda} = \lambda L^2/(E_{11}bh^3) \quad \text{for Material III}$$

Convergency study is, first, performed for the normalized fundamental frequencies and critical buckling loads. Results are given in Tables 1 and 2 for symmetrical $[0/90]_s$ and unsymmetrical [0/90] laminated beams with different boundary conditions. As can be seen, the present beam element converges rapidly when the number of elements increases. N = 8 elements seem to satisfy the required convergency for the analyses. Here, the results are also compared with the available ones. According to the tables, the results agree well with those of available literature except the normalized buckling load of C-C [0/90] beam for the considered case.

The normalized fundamental frequencies are presented for cross-ply and angle-ply laminated beams in Tables 3 and 4, respectively. Comparisons with the available results of

Table 1 Convergence study for normalized fundamental frequencies of laminated beams

Beam	N_e	S-S	C-C	C-F
$[0/90]_s$ L/h = 15 Material III	4	2.4901	4.6153	0.9243
	6	2.4896	4.6081	0.9242
	8	2.4895	4.6058	0.9241
	10	2.4895	4.6048	0.9241
	12	2.4895	4.6043	0.9241
	Analytical[1]	2.5015	4.6531	0.9251
[0/90] L/h = 10 Material I (E_1/E_2 = 40)	4	6.754	13.498	2.509
	6	6.753	13.474	2.508
	8	6.753	13.467	2.508
	10	6.753	13.464	2.508
	12	6.753	13.463	2.508
	Analytical[2]	6.945	13.670	2.543

[1] Parabolic shear deformation beam theory (Aydoğdu 2005)
[2] Higher-order theory based on trigonometric series (Nguyen *et al*. 2017)

Table 2 Convergence study for normalized buckling loads of laminated beams (Material I, E_1/E_2 = 40, L/h = 10)

Beam	N_e	S-S	C-C	C-F
$[0/90]_s$	4	17.731	33.169	6.2431
	6	17.726	33.111	6.2429
	8	17.725	33.100	6.2429
	10	17.725	33.097	6.2429
	12	17.725	33.096	6.2429
	FEM[1]	17.734	32.829	6.2459
[0/90]	4	4.676	13.411	1.304
	6	4.674	13.361	1.304
	8	4.674	13.352	1.304
	10	4.674	13.350	1.304
	12	4.674	13.349	1.304
	Analytical[2]	4.942	15.626	1.324

[1] Isogeometric finite element based on FSDT (Wang *et al*. 2015)
[2] Higher-order theory based on trigonometric series (Nguyen *et al*. 2017)

Table 3 Normalized fundamental frequencies of [0/90/0] and [0/90] laminated beams (Material I, E_1 / E_2 = 40)

BCs	Lay-up	Theory	L / h				
			5	10	20	30	50
S-S	[0/90/0]	Present	9.173	13.558	16.303	17.036	17.455
		Nguyen *et al*. (2017)	9.208	13.614	16.338	17.055	17.462
		Mantari and Canales (2016)	9.208	13.610	-	-	-
	[0/90]	Present	6.024	6.753	7.163	7.248	7.293
		Nguyen *et al*. (2017)	6.128	6.945	7.219	7.274	7.302
		Mantari and Canales (2016)	6.109	6.913	-	-	-
C-F	[0/90/0]	Present	4.154	5.474	6.064	6.195	6.266
		Nguyen *et al*. (2017)	4.234	5.498	6.070	6.198	6.267
		Mantari and Canales (2016)	4.221	5.490	-	-	-
	[0/90]	Present	2.277	2.508	2.581	2.596	2.603
		Nguyen *et al*. (2017)	2.383	2.543	2.591	2.600	2.605
		Mantari and Canales (2016)	2.375	2.532	-	-	-
C-C	[0/90/0]	Present	10.762	19.212	29.450	34.135	37.626
		Nguyen *et al*. (2017)	11.607	19.728	29.695	34.268	37.679
		Mantari and Canales (2016)	11.486	19.652	-	-	-
	[0/90]	Present	9.474	13.467	15.144	15.993	16.328
		Nguyen *et al*. (2017)	10.027	13.670	15.661	16.154	16.429
		Mantari and Canales (2016)	9.974	13.628	-	-	-

Table 4 Normalized fundamental frequencies of laminated beams with different lay-ups (Material I, E_1 / E_2 = 40)

L/h	Lay-up	S-S		C-F	
		Present	HSDT[1]	Present	HSDT[1]
5	[0/30/0]	9.4203	9.4651	4.2489	4.3218
	[0/45/0]	9.3393	9.3801	4.2155	4.2855
	[0/60/0]	9.2572	9.2946	4.1840	4.2519
	[0/±30/0]	9.3491	9.4194	4.2111	4.2821
	[0/±45/0]	9.2203	9.2928	4.1471	4.2129
	[0/±60/0]	9.0990	9.1699	4.0931	4.1548
	$[0/90]_2$	7.3168	7.7822	3.1799	3.3187
10	[0/30/0]	13.8312	13.8823	5.5622	5.5791
	[0/45/0]	13.7290	13.7795	5.5249	5.5412
	[0/60/0]	13.6383	13.6889	5.4953	5.5116
	[0/±30/0]	13.6569	13.7306	5.4821	5.4982
	[0/±45/0]	13.4316	13.5092	5.3834	5.3987
	[0/±60/0]	13.2580	13.3371	5.3142	5.3289
	$[0/90]_2$	9.9909	10.2007	3.8468	3.9002

[1] Mantari and Canales (2016)

analytical solutions based on HSDT given by Mantari and Canales (2016) and Nguyen *et al*. (2017) are made. As seen, the results are in good agreement. As the slenderness (L/h) increases, the natural frequencies increase, too.

In Table 5, the normalized buckling loads for [0/90/0] and [0/90] laminated composite beams with simple supports are given. For comparison, the analytical solutions given by Nguyen *et al*. (2017) and Aydogdu (2006), and the finite element solution given by Vo and Thai (2012), all based on HSDT, are considered. The results are in good agreement. The normalized buckling loads increase with increasing the slenderness (L/h).

In Tables 6 and 7, the normalized buckling loads for cross-ply and angle-ply laminated beams are compared to those of the analytical solutions based on HSDT given by Mantari and Canales (2016) and Nguyen *et al*. (2017). The present element agrees well with those of the higher-order theories considered with some exceptions. For the beams with [0/90] lamina stacking, the present element shows great discrepancy from the other solutions considered, i.e., S-S beams with L / h = 5 and C-C beams with L / h = 5 and 10.

Some further results for laminated composite beams are also given by Figs. 4 to 6. Effect of the fiber angle on the normalized fundamental frequencies and buckling loads are shown in Fig. 4. Unidirectional [θ] and unsymmetrical [0/θ] beams with Material III are considered. As seen, both the normalized frequencies and buckling loads decrease with increasing the fiber angle.

Fig. 5 shows the variation of the normalized frequencies and buckling loads with the slenderness for $[60/\text{-}60]_s$ beam with Material II and different end conditions. With increasing the slenderness, both the normalized frequencies and buckling loads increase.

Fig. 6 shows the effect of material anisotropy (E_1/E_2) on

Table 5 Normalized buckling loads of simply-supported [0/90/0] and [0/90] beams (Materials I and II, $E_1 / E_2 = 10$)

	Lay-up	Theory	L / h				
			5	10	20	30	50
Material I	[0/90/0]	Present	4.722	6.811	7.665	7.848	7.945
		Nguyen *et al*. (2017)	4.727	6.814	7.666	7.848	7.945
		Aydogdu (2006)	4.726	-	7.666	-	-
		Vo and Thai (2012)	4.709	6.778	7.620	-	7.896
	[0/90]	Present	1.890	2.155	2.238	2.254	2.262
		Nguyen *et al*. (2017)	1.920	2.168	2.241	2.255	2.262
		Aydogdu (2006)	1.919	-	2.241	-	-
		Vo and Thai (2012)	1.910	2.156	2.228	-	2.249
Material II	[0/90/0]	Present	3.447	5.969	7.368	7.706	7.892
		Nguyen *et al*. (2017)	3.728	6.206	7.460	7.751	7.909
		Aydogdu (2006)	3.728	-	7.459	-	-
		Vo and Thai (2012)	3.717	6.176	7.416	-	7.860
	[0/90]	Present	1.744	2.108	2.225	2.248	2.260
		Nguyen *et al*. (2017)	1.766	2.116	2.227	2.249	2.260
		Aydogdu (2006)	1.765	-	2.226	-	-
		Vo and Thai (2012)	1.758	2.104	2.214	-	2.247

Table 6 Normalized buckling loads of [0/90/0] and [0/90] laminated beams (Material I, $E_1 / E_2 = 40$)

BCs	Lay-up	Theory	L / h				
			5	10	20	30	50
S-S	[0/90/0]	Present	8.591	18.815	27.075	29.490	30.904
		Nguyen *et al*. (2017)	8.613	18.832	27.086	29.496	30.906
		Mantari and Canales (2016)	8.585	18.796	-	-	-
	[0/90]	Present	3.337	4.674	5.215	5.331	5.392
		Nguyen *et al*. (2017)	3.907	4.942	5.297	5.369	5.406
		Aydogdu (2006)	3.906	-	-	-	-
		Mantari and Canales (2016)	3.856	4.887	-	-	-
C-F	[0/90/0]	Present	4.704	6.769	7.610	7.790	7.886
		Nguyen *et al*. (2017)	4.708	6.772	7.611	7.790	7.886
		Mantari and Canales (2016)	4.673	6.757	-	-	-
	[0/90]	Present	1.168	1.304	1.343	1.351	1.355
		Nguyen *et al*. (2017)	1.236	1.324	1.349	1.353	1.356
		Aydogdu (2006)	1.235	-	-	-	-
		Mantari and Canales (2016)	1.221	1.311	-	-	-
C-C	[0/90/0]	Present	11.239	34.369	75.281	97.225	114.416
		Nguyen *et al*. (2017)	11.652	34.453	75.328	97.248	114.398
		Mantari and Canales (2016)	11.502	34.365	-	-	-
	[0/90]	Present	6.573	13.352	18.702	20.258	21.168
		Nguyen *et al*. (2017)	8.674	15.626	19.768	20.780	21.372
		Mantari and Canales (2016)	8.509	15.468	-	-	-

the normalized fundamental frequencies and buckling loads for $[0/90]_s$ and [0/90] composite beams with simple ends. As can be seen, the normalized frequencies and buckling loads increase with increasing the material anisotropy

(E_1/E_2). E_1/E_2 is more effective on $[0/90]_s$ beam compared to [0/90] one. In addition, $[0/90]_s$ beam has greater frequencies and buckling loads than those of [0/90] beam.

Table 7 Normalized buckling loads of laminated beams with different lay-ups (Material I, $E_1 / E_2 = 40$)

L/h	Lay-up	S-S		C-F	
		Present	HSDT[1]	Present	HSDT[1]
5	[0/30/0]	9.0679	9.0718	4.8976	4.8633
	[0/45/0]	7.8583	7.6533	4.8249	4.7909
	[0/60/0]	8.7522	8.7473	4.7606	4.7275
	[0/±30/0]	8.9658	8.9843	4.7894	4.7569
	[0/±45/0]	8.7202	8.7439	4.6332	4.6034
	[0/±60/0]	8.4903	8.5136	4.5139	4.4857
	$[0/90]_2$	5.5231	6.1626	2.5183	2.6416
10	[0/30/0]	19.5907	19.5591	6.9606	6.9473
	[0/45/0]	19.3003	19.2700	6.8727	6.8596
	[0/60/0]	19.0429	19.0166	6.8085	6.7963
	[0/±30/0]	19.1581	19.1350	6.7383	6.7246
	[0/±45/0]	18.5333	18.5228	6.4867	6.4746
	[0/±60/0]	18.0561	18.0533	6.3216	6.3106
	$[0/90]_2$	10.0733	10.5854	3.1911	3.2335

[1] Mantari and Canales (2016)

In Fig. 7, first three mode shapes of vibration for S-S, C-C and C-F beams with [0/90] lamina stacking obtained by the present element are given. As seen, with the present element, mode shapes can be obtained in their correct form.

4.2 Soft-core sandwich beams

Table 8 gives the normalized fundamental frequencies of a simple five-layer (0/90/core/0/90) soft-core sandwich beam with E_{11} = 131 GPa, E_{22} = 10.34 GPa, $G_{12} = G_{23}$ = 6.895 GPa, G_{13} = 6.205 GPa, ν_{12} = 0.22, ρ = 1627 kg/m^3 for face sheets, and $E_{11} = E_{22} = E_{33} = 6.89\times10^{-3}$ GPa, $G_{12} = G_{13} = G_{23} = 3.45\times10^{-3}$ GPa, ν_{12} = 0 for isotropic core. Here, t_c and t_f denote the thickness of core and face sheets, respectively. The natural frequencies are normalized as $\bar{\omega} = \omega L^2\sqrt{\rho/E_{22f}}/h$. The global-local higher-order theory (GLHT), the zig-zag theory (ZZT) and the higher-order shear deformation theory (HSDT) given by Zhen and Wanji (2008) are used for comparison. As seen, the results of the present element agree well with those of the work considered for different slenderness ratio. Our results are in a better agreement with that of ZZT which is a layer-wise theory.

Normalized buckling loads $\bar{\lambda} = \lambda L^2/(E_{2f}h^3)$ for a simply-supported soft-core sandwich beam according to the different beam theories are given in Table 9. Material properties are: E = 70 GPa and ν = 0.3 for isotropic aluminum face sheets, and $E_{11} = 1\times10^{-5}$ MPa, E_{22} = 109

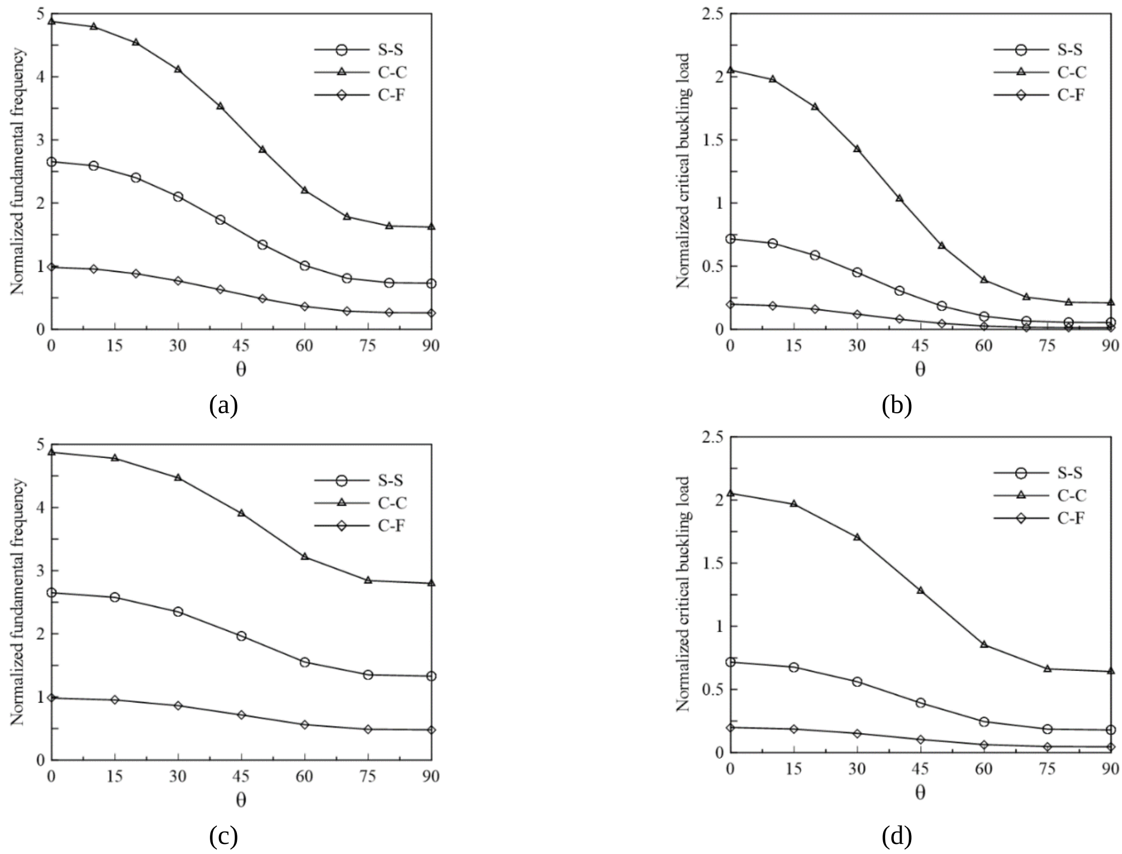

Fig. 4 Variation of the normalized fundamental frequencies and buckling loads with the fiber angle: (a) and (b) [θ] beam; (c) and (d) [0 / θ] beam (Material III, L / h = 15)

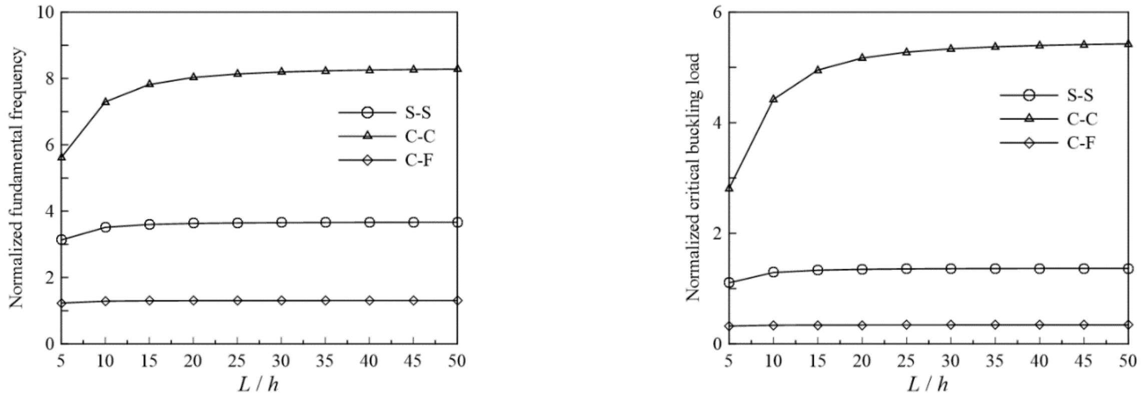

Fig. 5 Effect of the slenderness on the normalized fundamental frequencies and buckling loads for $[60/-60]_s$ composite beams (Material II, $E_1 / E_2 = 10$)

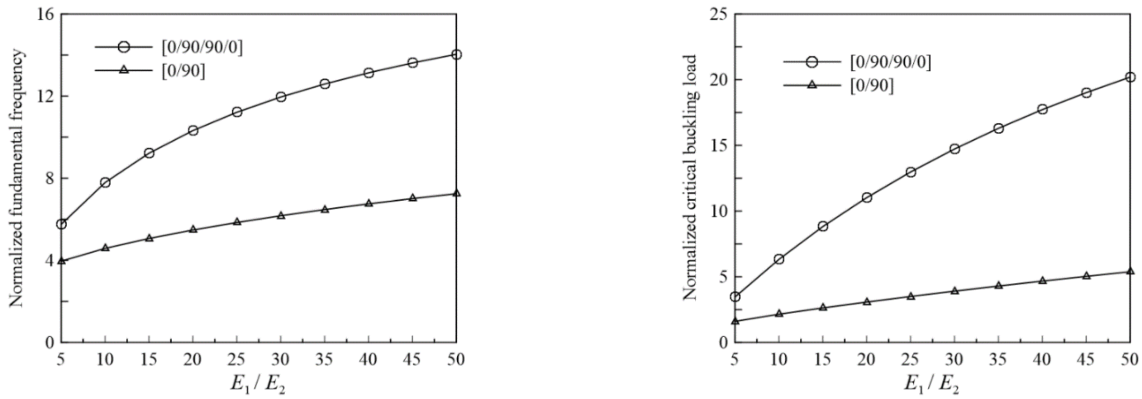

Fig. 6 Effect of material anisotropy on the normalized fundamental frequencies and buckling loads for [0/90/90/0] and [0/90] composite beams with simple ends (Material I, $L / h = 10$)

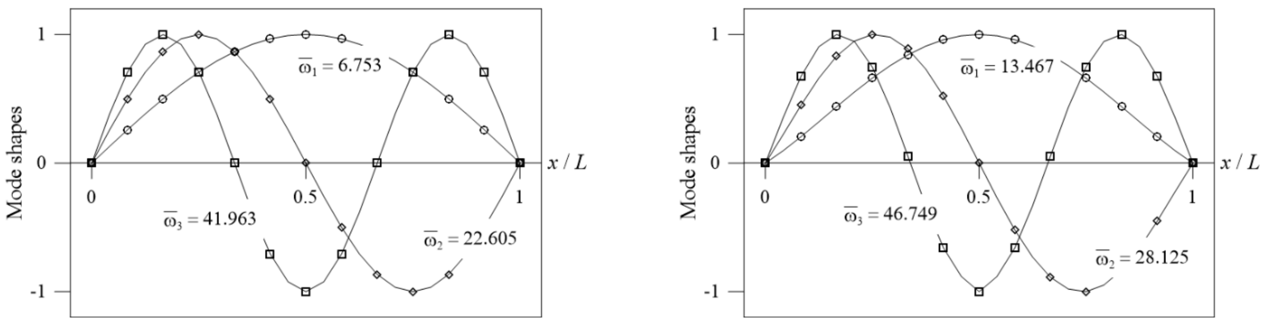

(a) S-S beam (b) C-C beam

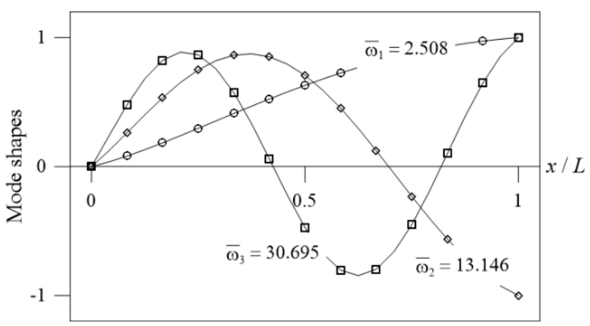

(c) C-F beam

Fig. 7 First three mode shapes of vibration for [0/90] laminated beams with various end conditions ($L/h = 10$, Material I, $E_1 / E_2 = 40$)

Table 8 Comparison of normalized fundamental frequencies for a soft-core sandwich beam (0/90/core/0/90, t_c / t_f = 10)

L / h	Present	ZZT[1]	GLHT[1]	HSDT[1]
2	0.4413	0.4430	0.4500	0.4560
4	0.6161	0.6161	0.6384	0.6547
10	1.2838	1.2822	1.3467	1.3956
20	2.4381	2.4347	2.5588	2.6533
30	3.5189	3.5141	3.6830	3.8107
40	3.4884	3.4824	4.6800	4.8280
50	5.3342	5.3272	5.5389	5.6960
60	6.0581	6.0503	6.2648	6.4223
70	6.6699	6.6616	6.8710	7.0233
80	7.1836	7.1747	7.3742	7.5180
90	7.6134	7.6042	7.7911	7.9249
100	7.9732	7.9637	8.1369	8.2602

[1] Zhen and Wanji (2008)

Table 9 Normalized buckling loads of simply-supported sandwich beams for different beam theories

t_c / t_f	L / h	Present	ZZT[1]	GLHT[1]	MLWT[2]
5	2	0.006748	0.006794	0.006719	0.006222
	5	0.01486	0.01486	0.01484	0.01432
	10	0.04183	0.04182	0.04182	0.041084
	50	0.3649	0.3648	0.3648	0.34319
	100	0.5023	-	-	0.46208
25	2	0.001601	0.001601	0.001601	0.0015299
	5	0.009143	0.009143	0.009142	0.0090314
	10	0.03169	0.03168	0.03168	0.031096
	50	0.1558	0.1558	0.1558	0.14385
	100	0.1776	-	-	0.16233
50	2	0.001510	0.001510	0.001510	0.0014419
	5	0.008693	0.008692	0.008692	0.0085553
	10	0.02758	0.02756	0.02756	0.026762
	50	0.09074	0.09072	0.09072	0.083230
	100	0.09775	-	-	0.089150

[1] Zhen and Wanji (2008); [2] Dafedar and Desai (2004);
[3] Kahya (2012)

MPa, G_{12} = 26.6 MPa, and $\nu_{12} = 1\times10^{-5}$ for orthotropic core. When the slenderness increases, the normalized buckling loads increase, too. However, they decrease with increasing the core-to-face thickness ratio. FSDT (Kahya 2012), GLHT and ZZT (Zhen and Wanji 2008), and the mixed layer-wise theory (MLWT) (Dafedar and Desai 2004) are used for comparison. The results are in good agreement. When the core-to-face thickness ratio increases, the perfect agreement is seen among the present element, ZZT and GLHT.

5. Conclusions

A multi-layer layer-wise finite element for vibration and buckling analyses of laminated composite and sandwich beams based on a higher-order theory is presented. Slip and delamination between the layers are not allowed. Element matrices are derived through the Lagrange's equations. Numerical results have been obtained by a computer program written by the authors in FORTRAN language.

According to the results of the study, the following conclusions can be drawn:

- Compared to other higher-order theories available in the literature, the present element's accuracy in calculation of natural frequencies and buckling loads of laminated composite and sandwiched beams is very good.
- It is observed that the element presented here has some exceptions in calculating buckling loads. For unsymmetric cross-ply [0/90/…] beams with C-C and S-S end conditions in case of L / h < 10, the present element gives erroneous results compared to the available literature considered here. Authors think that this may be due to some material coupling for this type of lamina configuration, and if the out-off plane displacement component (v) is taken into account in the kinematic relations, we will have obtained more accurate results.
- Since the present element is constituted in a layer-wise manner, it can be suitable for the solution of slip and delamination problems of laminated beams, which is a further work of the authors.

References

Arya, H. (2003), "A new zig-zag model for laminated composite beams: free vibration analysis", *J. Sound Vib.*, **264**, 485-490.

Aydogdu, M. (2005), "Vibration analysis of cross-ply laminated beams with general boundary conditions by Ritz method", *Int. J. Mech. Sci.*, **47**(11), 1740-1755.

Aydogdu, M. (2006), "Buckling analysis of cross-ply laminated beams with general boundary conditions by Ritz method", *Compos. Sci. Technol.*, **66**(10), 1248-1255.

Banerjee, J.R. (1998), "Free vibration of axially loaded composite Timoshenko beams using the dynamic stiffness matrix method", *Comput. Struct.*, **69**(2), 197-208.

Chakrabarti, A., Chalak, H.D., Iqbal, M.A. and Sheikh, A.H. (2012), "Buckling analysis of laminated sandwich beam with soft core", *Latin Am. J. Solids Struct.*, **9**(3), 1-15.

Chakraborty, A., Mahapatra, R.D. and Gopalakrishan, S. (2002), "Finite element analysis of free vibration and wave propagation in asymmetric composite beams with structural discontinuities", *Compos. Struct.*, **55**(1), 23-36.

Dafedar, J.B. and Desai, Y.M. (2004), "Stability of composite and sandwich struts by mixed formulation", *ASCE J. Eng. Mech.*, **130**(7), 762-770.

Filippi, M. and Carrera, E. (2016), "Bending and vibrations analyses of laminated beams by using a zig-zag-layer-wise theory", *Compos. Part B: Eng.*, **98**, 269-280.

Goyal, V.K. and Kapania, R.K. (2007), "A shear-deformable beam element for the analysis of laminated composites", *Finite Elem. Anal. Des.*, **43**(6-7), 463-477.

Jafari-Talookolaei, R.A., Abedi, M., Kargarnovin, M.H. and Ahmadian M.T. (2012), “An analytical approach for the free vibration analysis of generally laminated composite beams with shear effect and rotary inertia”, *Int. J. Mech. Sci.*, **65**(1), 97-104.

Kahya, V. (2012), “Dynamic analysis of laminated composite beams under moving loads using finite element method”, *Nuclear Eng. Des.*, **243**, 41-48.

Kahya, V. (2016), “Buckling analysis of laminated composite and sandwich beams by the finite element method”, *Compos. Part B: Eng.*, **91**, 126-134.

Kant, T., Marur, S.R. and Rao, G.S. (1998), “Analytical solution to the dynamic analysis of laminated beams using higher order refined theory”, *Compos. Struct.*, **40**(1), 1-9.

Karama, M., Abou Harb, B., Mistou, S. and Caperaa, S. (1998), “Bending, buckling and free vibration of laminated composite with a transverse shear stress continuity model”, *Compos. Part B: Eng.*, **29**(3), 223-234.

Li, Z.M. and Qiao, P. (2015), “Buckling and postbuckling behavior of shear deformable anisotropic laminated beams with initial geometric imperfections subjected to axial compression”, *Eng. Struct.*, **85**, 277-292.

Mantari, J.L. and Canales, F.G. (2016), “Free vibration and buckling of laminated beams via hybrid Ritz solution for various penalized boundary conditions”, *Compos. Struct.*, **152**, 306-315.

Matsunaga, H. (2001), “Vibration and buckling of multilayered composite beams according to higher order deformation theories”, *J. Sound Vib.*, **246**(1), 47-62.

Nguyen, T.K., Nguyen, N.D., Vo, T.P. and Thai, H.T. (2017), “Trigonometric-series solution for analysis of laminated composite beams”, *Compos. Struct.*, **160**, 142-151.

Rao, K.M., Desai, Y.M. and Chitnis, M.R. (2001), “Free vibrations of laminated beams using mixed theory”, *Compos. Struct.*, **52**(2), 149-160.

Reddy, J.N. (1997), *Mechanics of Laminated Composite Plates: Theory and Analysis*, CRC Press, Boca Raton, FL, USA.

Teboub, Y. and Hajela, P. (1995), “Free vibration of generally layered composite beams using symbolic computations”, *Compos. Struct.*, **33**, 123-134.

Vo, T.P. and Thai, H.T. (2012), “Vibration and buckling of composite beams using refined shear deformation theory”, *Int. J. Mech. Sci.*, **62**(1), 67-76.

Wang, X., Zhu, X. and Hu, P. (2015), “Isogeometric finite element method for buckling analysis of generally laminated composite beams with different boundary conditions”, *Int. J. Mech. Sci.*, **104**, 190-199.

Yuan, F.G. and Miller, R.E. (1989), “A new finite element for laminated composite beams”, *Comput. Struct.*, **31**(5), 737-745.

Yuan, F.G. and Miller, R.E. (1990), “A higher-order finite element for laminated beams”, *Compos. Struct.*, **14**(2), 125-150.

Zhen, W. and Wanji, C. (2008), “An assessment of several displacement theories for the vibration and stability analysis of laminated composite and sandwich beams”, *Compos. Struct.*, **84**(4), 337-349.

CC

Appendix

The elements of the mass, stiffness and geometric stiffness matrices are given below, respectively

$$\mathbf{m} = \begin{bmatrix} \mathbf{m}_{11} & \mathbf{0} & \mathbf{0} & \mathbf{m}_{14} & \mathbf{0} \\ & \mathbf{m}_{22} & \mathbf{0} & \mathbf{0} & \mathbf{0} \\ & & \mathbf{m}_{33} & \mathbf{0} & \mathbf{m}_{35} \\ & & & \mathbf{m}_{44} & \mathbf{0} \\ sym. & & & & \mathbf{m}_{55} \end{bmatrix},$$

$$\mathbf{k} = \begin{bmatrix} \mathbf{k}_{11} & \mathbf{0} & \mathbf{0} & \mathbf{k}_{14} & \mathbf{0} \\ & \mathbf{k}_{22} & \mathbf{k}_{23} & \mathbf{0} & \mathbf{k}_{25} \\ & & \mathbf{k}_{33} & \mathbf{0} & \mathbf{k}_{35} \\ & & & \mathbf{k}_{44} & \mathbf{0} \\ sym. & & & & \mathbf{k}_{55} \end{bmatrix}, \qquad (A1)$$

$$\mathbf{g} = \begin{bmatrix} \mathbf{0} & \mathbf{0} & \mathbf{0} & \mathbf{0} & \mathbf{0} \\ & \mathbf{g}_{22} & \mathbf{0} & \mathbf{0} & \mathbf{0} \\ & & \mathbf{0} & \mathbf{0} & \mathbf{0} \\ & & & \mathbf{0} & \mathbf{0} \\ sym. & & & & \mathbf{0} \end{bmatrix}$$

where

$$\mathbf{m}_{11} = \begin{bmatrix} 224\gamma_0 & 112\gamma_0 & -56\gamma_0 \\ 112\gamma_0 & 896\gamma_0 & 112\gamma_0 \\ -56\gamma_0 & 112\gamma_0 & 224\gamma_0 \end{bmatrix},$$

$$\mathbf{m}_{14} = \begin{bmatrix} -224\gamma_2 & -112\gamma_2 & 56\gamma_2 \\ -112\gamma_2 & -896\gamma_2 & -112\gamma_2 \\ 56\gamma_2 & -112\gamma_2 & -224\gamma_2 \end{bmatrix},$$

$$\mathbf{m}_{22} = \begin{bmatrix} 128\gamma_0 & 99\gamma_0 & -36\gamma_0 & 19\gamma_0 \\ 99\gamma_0 & 648\gamma_0 & -81\gamma_0 & -36\gamma_0 \\ -36\gamma_0 & -81\gamma_0 & 648\gamma_0 & 99\gamma_0 \\ 19\gamma_0 & -36\gamma_0 & 99\gamma_0 & 128\gamma_0 \end{bmatrix},$$

$$\mathbf{m}_{33} = \begin{bmatrix} 224\gamma_2 & 112\gamma_2 & -56\gamma_2 \\ 112\gamma_2 & 896\gamma_2 & 112\gamma_2 \\ -56\gamma_2 & 112\gamma_2 & 224\gamma_2 \end{bmatrix}, \qquad (A2)$$

$$\mathbf{m}_{35} = \mathbf{m}_{44} = \begin{bmatrix} 224\gamma_4 & 112\gamma_4 & -56\gamma_4 \\ 112\gamma_4 & 896\gamma_4 & 112\gamma_4 \\ -56\gamma_4 & 112\gamma_4 & 224\gamma_4 \end{bmatrix},$$

$$\mathbf{m}_{55} = \begin{bmatrix} 224\gamma_6 & 112\gamma_6 & -56\gamma_6 \\ 112\gamma_6 & 896\gamma_6 & 112\gamma_6 \\ -56\gamma_6 & 112\gamma_6 & 224\gamma_6 \end{bmatrix}$$

$$\mathbf{k}_{11} = \begin{bmatrix} 7\alpha_0 & -8\alpha_0 & \alpha_0 \\ -8\alpha_0 & 16\alpha_0 & -8\alpha_0 \\ \alpha_0 & -8\alpha_0 & 7\alpha_0 \end{bmatrix},$$

$$\mathbf{k}_{14} = \begin{bmatrix} -7\alpha_2 & 8\alpha_2 & -\alpha_2 \\ 8\alpha_2 & -16\alpha_2 & 8\alpha_2 \\ -\alpha_2 & 8\alpha_2 & -7\alpha_2 \end{bmatrix},$$

$$\mathbf{k}_{22} = \begin{bmatrix} 444\beta_0 & -567\beta_0 & 162\beta_0 & -39\beta_0 \\ -567\beta_0 & 1296\beta_0 & -891\beta_0 & 162\beta_0 \\ 162\beta_0 & -891\beta_0 & 1296\beta_0 & -567\beta_0 \\ -39\beta_0 & 162\beta_0 & -567\beta_0 & 444\beta_0 \end{bmatrix},$$

$$\mathbf{k}_{23} = \begin{bmatrix} 83L\beta_0 & 44L\beta_0 & -7L\beta_0 \\ -99L\beta_0 & 108L\beta_0 & -9L\beta_0 \\ 9L\beta_0 & -108L\beta_0 & 99L\beta_0 \\ 7L\beta_0 & -44L\beta_0 & -83L\beta_0 \end{bmatrix},$$

$$\mathbf{k}_{25} = \begin{bmatrix} 249L\beta_2 & 132L\beta_2 & -21L\beta_2 \\ -297L\beta_2 & 324L\beta_2 & -27L\beta_2 \\ 27L\beta_2 & -324L\beta_2 & 297L\beta_2 \\ 21L\beta_2 & -132L\beta_2 & -249L\beta_2 \end{bmatrix}, \qquad (A2)$$

$$\mathbf{k}_{33} = \begin{bmatrix} 7\alpha_2 + 16L^2\beta_0 & -8\alpha_2 + 8L^2\beta_0 & \alpha_2 - 4L^2\beta_0 \\ -8\alpha_2 + 8L^2\beta_0 & 16\alpha_2 + 64L^2\beta_0 & -8\alpha_2 + 8L^2\beta_0 \\ \alpha_2 - 4L^2\beta_0 & -8\alpha_2 + 8L^2\beta_0 & 7\alpha_2 + 16L^2\beta_0 \end{bmatrix},$$

$$\mathbf{k}_{35} = \begin{bmatrix} 7\alpha_4 + 48L^2\beta_2 & -8\alpha_4 + 24L^2\beta_2 & \alpha_4 - 12L^2\beta_2 \\ -8\alpha_4 + 24L^2\beta_2 & 16\alpha_4 + 192L^2\beta_2 & -8\alpha_4 + 24L^2\beta_2 \\ \alpha_4 - 12L^2\beta_2 & -8\alpha_4 + 24L^2\beta_2 & \alpha_4 + 48L^2\beta_2 \end{bmatrix},$$

$$\mathbf{k}_{44} = \begin{bmatrix} 7\alpha_4 + 64L^2\beta_2 & -8\alpha_4 + 32L^2\beta_2 & \alpha_4 - 16L^2\beta_2 \\ -8\alpha_4 + 32L^2\beta_2 & 16\alpha_4 - 256L^2\beta_2 & -8\alpha_4 + 32L^2\beta_2 \\ \alpha_4 - 16L^2\beta_2 & -8\alpha_4 + 32L^2\beta_2 & 7\alpha_4 + 64L^2\beta_2 \end{bmatrix},$$

$$\mathbf{k}_{55} = \begin{bmatrix} 7\alpha_6 + 144L^2\beta_4 & -8\alpha_6 + 72L^2\beta_4 & \alpha_6 - 36L^2\beta_4 \\ -8\alpha_6 + 72L^2\beta_4 & 16\alpha_6 + 576L^2\beta_4 & -8\alpha_6 + 72L^2\beta_4 \\ \alpha_6 - 36L^2\beta_4 & -8\alpha_6 + 72L^2\beta_4 & 7\alpha_6 + 144L^2\beta_4 \end{bmatrix} \qquad (A3)$$

$$\mathbf{g}_{22} = \begin{bmatrix} 444S_n & -567S_n & 162S_n & -39S_n \\ -567S_n & 1296S_n & -891S_n & 162S_n \\ 162S_n & -891S_n & 1296S_n & -567S_n \\ -39S_n & 162S_n & -567S_n & 444S_n \end{bmatrix} \qquad (A4)$$

In above, α_n, β_n, γ_n and S_n are given by

$$\alpha_n = \frac{\bar{Q}_{11}A_n}{3L}, \quad \beta_n = \frac{\bar{Q}_{55}A_n}{120L}, \quad \gamma_n = \frac{\rho L A_n}{1680}, \quad S_n = \frac{1}{120L} \quad (n = 0,2,4,6) \qquad (A5)$$

where L is the element length, ρ is the density of beam, and A_n is the integral over the cross-sectional area given by

$$A_n = \int_A z^n \, \mathrm{dA} \qquad (A6)$$

For layers with a rectangular cross-section with a width b and height h

$$A_0 = bh, \quad A_2 = \frac{bh^3}{12}, \quad A_4 = \frac{bh^5}{80}, \quad A_6 = \frac{bh^7}{448} \qquad (A7)$$